Measuring Changes in the Fundamental Constants with Redshifted Radio Absorption Lines

S. J. Curran[a], N. Kanekar[b], J. K. Darling[c]

[a]School of Physics, University of New South Wales, Sydney, Australia

[b]Kapteyn Institute, University of Groningen, The Netherlands

[c]Carnegie Observatories, Pasadena, USA

Strong evidence has recently emerged for a variation in the fine structure constant, $\alpha \equiv e^2/\hbar c$, over the history of the Universe. This was concluded from a detailed study of the relative positions of redshifted optical quasar absorption spectra. However, *radio* absorption lines at high redshift offer a much higher sensitivity to a cosmological change in α than optical lines. Furthermore, through the comparison of various radio transitions, H I, OH and millimetre molecular (e.g. CO) lines, any variations in the proton g-factor, g_p, and the ratio of electron/proton masses, $\mu \equiv m_e/m_p$, may also be constrained. Presently, however, systems exhibiting redshifted radio lines are rare with the bias being towards those associated with optically selected QSOs. With its unprecedented sensitivity, large bandwidth and wide field of view, the SKA will prove paramount in surveying the sky for absorbers unbiased by dust extinction. This is expected to yield whole new samples of H I and OH rich systems, the latter of which will prove a useful diagnostic in finding redshifted millimetre absorbers. As well as uncovering many new systems through these blind surveys, the SKA will enable the detection of H I absorption in many more of the present optical sample – down to column densities of $\sim 10^{17}$ cm^{-2}, or $\gtrsim 2$ orders of magnitude the sensitivity of the current limits. Armed with these large samples together with the high spectral resolutions, available from the purely radio comparisons, the SKA will provide statistically sound measurements of the values of these fundamental constants in the early Universe, thus providing a physical test of Grand Unified Theories.

1. INTRODUCTION

Much interest has recently centered on the possibility that fundamental constants such as the fine structure constant might vary with cosmic time. Many theoretical models, such as superstring theories (presently the best candidate to unify gravity and the other fundamental interactions) and Kaluza-Klein theories, *naturally predict a spatio-temporal variation of these constants*. Such models usually invoke extra dimensions compactified on tiny scales, with the fundamental constants arising as functions of the scale lengths of these extra dimensions (e.g. [37, 14]). At present, no mechanism has been found to keep the compactified scale-lengths constant implying that, if extra dimensions exist and their sizes undergo cosmological evolution, the three dimensional coupling constants should vary with time (e.g. [34]). Several other modern theories also provide strong motivation for an experimental search for variation in the fine structure constant (e.g. [63, 21]). Interestingly, varying constants provide alternative solutions to cosmological fine-tuning problems, such as the "flatness problem" and the "horizon problem" [47].

From terrestrial experiments, [20] find $\Delta\alpha/\alpha < 1.2 \times 10^{-7}$, whereas $\geq 4.5 \times 10^{-8}$ is found by [31], each from isotopic abundances measured in the Oklo natural fission reactor. This is 1.8×10^9 years old, corresponding to a redshift of $z \sim 0.1$.

However, astrophysical studies of redshifted spectral lines provide a powerful probe of putative changes in fundamental constants over a large fraction of the age of the Universe (e.g. [52, 3, 23, 48]): Recent studies of the relative redshifts of metal-ion atomic resonance transitions in the optical (Keck/HIRES) quasar spectra of 143 heavy element absorption systems are consistent with a smaller fine structure constant in the

intervening absorption clouds over the redshift range $0.2 < z_{\rm abs} < 3.7$ (Fig.1). However, since

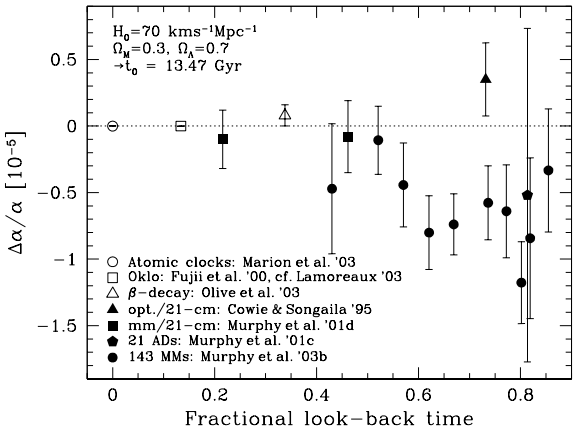

Figure 1. Summary of the previous measurements of $\Delta\alpha/\alpha$. The open symbols are local constraints [20, 31, 38, 44] and the filled symbols are QSO absorption constraints from the alkali doublet [43], the many-multiplet [40] and the radio methods (discussed in this chapter). Courtesy of Michael Murphy.

all of the observations which suggest a change in α use the same telescope and instrument [40], despite our best efforts [41], unforeseen systematic effects cannot be ruled out. Furthermore, [6] find no such variation from VLT/UVES data of 23 systems ($0.4 < z_{\rm abs} < 2.3$). Given the implications for theoretical physics, it is clear that independent checks are required which can refute or confirm the optical results. In particular, radio studies offer:

1. A different technique of potentially much higher accuracy than the purely optical methods.
2. The ability to study the evolution of other dimensionless fundamental constants, besides α.

Currently, however, the paucity of systems exhibiting HI 21 cm together with rotational or optical absorption severely limits our ability to carry out statistically sound comparisons. In this chapter we shall discuss how the SKA is expected to significantly increase the number of high redshift radio absorbers from which detailed study can greatly improve constraints in the cosmological variation in the fine structure constant, the ratio of electron–proton mass, and the proton g-factor.

2. RADIO LINES & FUNDAMENTAL CONSTANTS

Spectral lines such as the H I 21 cm line, cm-wave OH lines and mm-wave CO and HCO^+ lines arise from different physical mechanisms and hence have different dependences on these constants (e.g. [15, 8, 42, 29]). Further, the spectral resolution commonly available in radio spectroscopy is typically far better than that obtained in the optical domain, allowing higher precision redshift measurements.

Consider two transitions, with rest frequencies $\nu_1(z)$ and $\nu_2(z)$ that depend on redshift through their (different) dependences on certain fundamental constants. The ratio of the two frequencies, $y\,(\alpha, g_p, \mu, ...) \equiv \nu_1/\nu_2$ will vary with redshift as:

$$\frac{\Delta y}{y} = \frac{y\,(z) - y_0}{y_0} \approx \frac{\Delta z}{1+z_1} = \frac{z_2 - z_1}{1+z_1}, \qquad (1)$$

where z_1 and z_2 are the *measured* redshifts of the two lines in a given object and y_0 is the value of the ratio at the present epoch. One could thus, in principle, compare the redshift of an object as measured from the H I 21 cm, OH, and millimetre transitions, as well as the optical fine structure lines, in order to determine the evolution of combinations of different constants. Clearly, this must be carried out on a statistically large sample of objects in order to average out any intrinsic velocity offsets between the different species or differing lines of sight between the mm-wave and cm-wave continua.

2.1. Atomic Lines

The H I 21 cm line arises from a hyperfine spin-flip transition (ν_{21} = 1420.406 MHz), produced by the interaction of the magnetic fields of the electron and proton. The line frequency has the

dependence

$$\nu_{21} \propto g_p \mu \alpha^2 R_\infty \ , \quad (2)$$

where $R_\infty \equiv m_e e^4/\hbar^3 c$ is the Rydberg constant[1]. By comparison, the frequency of the optical transitions, governed by Coulombic interactions, are

$$\nu_{\rm opt} \propto (1 + 0.03\alpha^2) R_\infty, \quad (3)$$

thus we see that the spin-flip transition is ≈ 30 times as sensitive than the optical resonance transition to a given change in α [17]. The ratio of frequencies is

$$\frac{\nu_{21}}{\nu_{\rm opt}} \propto \mu \alpha^2 g_p, \quad (4)$$

(e.g. [10]), and so increasing the number of cosmologically distant QSO absorption systems with both optical and 21 cm lines would result in a significant improvement in measuring any cosmological changes in $\mu\alpha^2 g_p$.

2.2. Molecular Lines

2.2.1. Centimetre-wave OH lines

Cm-wave OH lines allow the interesting possibility of simultaneously measuring changes in α, g_p and μ, using spectral lines of a *single species* [15, 8, 29]. This is because these lines arise from two entirely different physical mechanisms, Lambda-doubling and hyperfine splitting [49], which have different dependences on the above constants: Each OH state gives rise to four cm-wave lines, allowing the possibility of multiple, independent estimates of any cosmological evolution. The strongest transitions are found in the ground state, at frequencies of $\nu_{\rm rest} =$ 1665.402 MHz and 1667.359 MHz ("main" lines) and 1612.231 MHz and 1720.530 MHz ("satellite" lines). At present, these are the only Lambda-doubled lines to have been detected at cosmological distances [7, 27] and hence, the best candidates for searches at higher redshifts with the SKA. It should be emphasized, however, that the SKA will cover the frequencies of *all* known Lambda-doubled OH lines (i.e. rest frequencies of 1.6 to 13 GHz) with high sensitivity.

[1]Note that the frequencies of all transitions discussed here are proportional to R_∞. Since this cancels out when comparing frequency ratios, it is usually not quoted in the literature.

An interesting aspect of the OH lines is the fact that various line frequency differences depend on all three of the above constants, while the frequency sums only depend on α and μ. For example, in the case of the ground state 18 cm lines, we have [8]

$$\nu_{1665} + \nu_{1667} \propto \mu^{2.57} \alpha^{-1.14}, \quad (5)$$

$$\nu_{1667} - \nu_{1665} \propto \mu^{2.44} \alpha^{-0.88} g_p, \quad (6)$$

$$\nu_{1720} - \nu_{1612} \propto \mu^{0.72} \alpha^{2.56} g_p, \quad (7)$$

where we see that Equations (5) and (7) have very different dependences on both α and μ, giving the ratio of the two frequencies a high sensitivity to changes in their numerical values.

In the next excited state, $^2\Pi_{1/2}$ $J = 1/2$, only the 4750.656 MHz main line is allowed (the $F = 0 \rightarrow 0$ main line is forbidden). This has the dependence [29]

$$\nu_{4750} \propto \mu^{0.51} \alpha^{2.98} R_\infty \ . \quad (8)$$

Again, Equations (5) and (8) have very different dependences on α and μ: In fact, their ratio is proportional to $\alpha^{4.12}$, one of the most sensitive to a change in the fine structure constant.

2.2.2. Millimetre-wave molecular lines

Mm-wave molecular lines from species such as CO, HCO^+, etc. arise from rotational transitions (e.g. [57]), with line frequencies proportional to μR_∞, thus providing a useful "anchor" with which to compare the H I and OH transitions. The high spectral resolution available makes millimetre lines potentially very useful and they may be compared with the 21 cm line giving [16]

$$\frac{\nu_{21}}{\nu_{\rm mm}} \propto \alpha^2 g_p, \quad (9)$$

or with the OH lines, giving

$$\frac{\nu_{1667}}{\nu_{\rm mm}} \propto \mu^{1.57} \alpha^{-1.14} \ , \ \frac{\nu_{4750}}{\nu_{\rm mm}} \propto \mu^{-0.49} \alpha^{2.98}. \quad (10)$$

Regarding these last constraints, a fairly tight linear correlation has been found between HCO^+ and OH column densities, both in the Galaxy [35] and out to $z \sim 1$ [27], extending over more than two orders of magnitude in column density. This

suggests that HCO^+ and OH are likely to be located in the same region of a molecular cloud, reducing the likelihood of velocity offsets between the two species. Similarly, [16] demonstrated a correlation between the individual velocity components of 21 cm and HCO^+ absorption along 9 lines of sight in the Galaxy, with a dispersion of 1.2 km s^{-1}.

2.3. Present radio results

Only four redshifted radio molecular absorbers are presently known: $z_{\rm abs} = 0.247$ toward PKS 1413+135; $z_{\rm abs} = 0.674$ toward B3 1504+377; $z_{\rm abs} = 0.685$ toward B0218+357; and $z_{\rm abs} = 0.889$ toward PKS 1830–210. The H I 21 cm [4, 5, 1, 7], millimetre (e.g. CO) [57, 54, 55, 58] and 18 cm OH main lines [7, 27] have been detected in all these systems while the 18 cm OH satellite lines have only been detected towards PKS 1413+135 [29]. These satellite lines have a clear velocity offset (≈ 12 km s^{-1}) from the main OH, H I and mm-wave lines. Further, the current H I and OH spectra toward PKS 1830–210 and B3 1504+377 have fairly poor velocity resolutions ($\gtrsim$ 10 km s^{-1} [27, 7, 2]), giving low accuracy measurements. As a result, constraints on changes in different combinations of fundamental constants are only available from the lines of sight toward PKS 1413+135 and B0218+357:

1. By comparing VLBA H I 21 cm redshifts with those obtained from the CO line, [3] obtained $\Delta x/x = (1 \pm 0.3) \times 10^{-5}$ at $z_{\rm abs} = 0.685$ towards B0218+357 and $\Delta x/x = (1.3 \pm 0.08) \times 10^{-5}$, where $x \equiv g_p \alpha^2$, at $z \sim 0.247$ towards PKS 1413+135.

2. The redshift of the sum of OH 1665 and 1667 MHz lines toward B0218+357 is in agreement with both the H I 21 cm and HCO^+ redshifts [8] and gives the constraint $\Delta x_1/x_1 = (-3.5 \pm 4.4) \times 10^{-6}$ (comparing H I and OH) and $\Delta x_2/x_2 = (6.5 \pm 3.3) \times 10^{-6}$ (comparing HCO^+ and OH), where $x_1 = \mu^{1.571} \alpha^{-3.141} g_p^{-1}$ and $x_2 = \mu^{1.571} \alpha^{-1.141}$.

   Note that only statistical errors are included in these estimates: [3] estimate further systematic errors of $\approx 2 \times 10^{-5}$ towards both B0218+357 and PKS 1413+135, arising from small-scale motions of $\sim$ 10 km s^{-1} .

3. [42] carried out a simultaneous fitting of the single dish H I and HCO^+ profiles to obtain $\Delta x/x = (-0.20 \pm 0.44) \times 10^{-5}$ towards PKS 1413+135 and $\Delta x/x = (-0.16 \pm 0.54) \times 10^{-5}$ towards B0218+357, where $x \equiv g_p \alpha^2$.

4. Finally, [30] have used the conjugate nature of the 1720 and 1612 MHz satellite lines toward PKS 1413+135 to argue that they arise in the same gas and obtained $\Delta x/x = (2.2 \pm 3.8) \times 10^{-5}$, where $x \equiv g_p [\alpha^2/y]^{1.849}$.

In addition to these purely radio results, the best current constraint from 21 cm and optical comparisons is from the $z_{\rm abs} = 1.77$ absorber towards QSO 1331+170, which gives $\Delta x/x = 0.7 \pm 1.1 \times 10^{-5}$ ($\Delta x/x \equiv \alpha^2 g_p \mu$, [10][2]).

In summary, the current radio studies exhibit no fractional changes in the fundamental constants of $\gtrsim 10^{-5}$ to $z_{\rm abs} \sim 0.7$, which is not inconsistent with the optical results.

3. PROSPECTS WITH THE SKA

3.1. Technical Considerations

The primary reason for the relatively few estimates (or constraints) of changes in different fundamental constants in the radio regime has been the small number of systems in which radio absorption has been so far detected (§2.3). As previously noted, radio molecular absorption (CO, HCO^+, OH, etc) has so far only been detected in four cosmologically distant absorbers, with the highest redshift absorber at $z_{\rm abs} \sim 0.9$ [58, 7]. Although the situation is somewhat better for 21 cm line absorption (see §3.2), only a handful of absorbers are known at intermediate redshifts, with just two confirmed detections at $z_{\rm abs} > 2.1$ [2, 50].

There are three main reasons for the small size of the radio absorber sample; low sensitivity,

[2]Again, the error is statistical assuming that no velocity offset exists between the optical and radio absorbers.

limited frequency coverage and severe radio frequency interference (RFI). While the former two factors affect observations at all radio bands, the latter is especially detrimental to observations of H I 21 cm and OH 18 cm lines which are redshifted to $\lesssim$ 1 GHz, a range strongly contaminated by terrestrial interference. Regarding the SKA:

1. Sensitivity: The H I 21 cm and OH transitions are far weaker than the optical resonance lines. The high sensitivity of the SKA is thus a critical factor in the detection of new redshifted absorption systems. This is also crucial for the precise measurements of the absorption redshifts of the different transitions. The current specifications for the sensitivity are

   (a) $A_{\rm eff}/T_{\rm sys} = 5000$ at 200 MHz, giving an r.m.s. noise of $\sigma = 0.2$ mJy,

   (b) $A_{\rm eff}/T_{\rm sys} = 20000$ at 0.5 to 5 GHz, giving $\sigma = 0.04$ mJy,

   (c) $A_{\rm eff}/T_{\rm sys} = 10000$ at 25 GHz, giving $\sigma = 0.01$ mJy,

   per 1 km s^{-1} channel after one hour of integration. By comparison, the most sensitive current low frequency interferometer, the GMRT, would have to integrate for $\approx$ 650 hours at P-band to reach similar noise levels.

2. Frequency and sky coverage: The SKA will provide uniform frequency coverage from $\approx$ 100 MHz to $\approx$ 25 GHz [24]. That is, it will be sensitive to H I 21 cm absorption and ground state 18 cm OH absorption at redshifts of $z \lesssim 13$ and $z \lesssim 16$, respectively. This coverage also gives HCO^+ and CO $J = 0 \rightarrow 1$ absorption at redshifts $z \gtrsim 2.6$ and $z \gtrsim 3.6$, respectively.

   The wide-band correlator will provide 10^4 channels over a bandwidth 25% of the band centre frequency [24]. In combination with its unrivaled low frequency coverage and the very wide field of view (200 square degrees at 0.7 GHz [24]), this will enable highly efficient blind surveys for H I and OH absorption, never before possible with an interferometer.

3. RFI: Terrestrial interference has long been the bugbear of searches for spectral lines at low frequencies, which lie outside the protected radio bands. This is particularly severe for systems at high redshift, for which the H I and OH ground state lines lie below 1 GHz, where TV and radio stations, mobile phones, navigation systems, etc. make these frequency ranges a veritable "RFI-forest". With its remote location and modern RFI mitigation techniques (such as beam nulling), the SKA is expected to reach theoretical noise levels in unprotected radio bands.

4. Resolution: The SKA will have an angular resolution of $\leq 0.02/\nu_{\rm GHz}$ arc-sec [24]. This will allow one to spatially map the H I and OH absorption, ensuring that comparisons between different lines are made for similar lines of sight. Furthermore, lines of sight towards different source components will provide independent measurements of changes in the three constants, α, g_p and μ.

3.2. Possible Targets

Of all the known radio transitions, 21 cm is, not surprisingly, the most commonly detected at high redshift (cf. §2.3). Known redshifted 21 cm absorbers can be broadly separated into three classes:

1. Damped Lyman-alpha absorption systems (DLAs) due to intervening galaxies ([28] and references therein).

2. H I clouds associated with the QSO host (e.g. [4, 2, 25, 22, 51]).

3. Gravitational lenses (e.g. [39, 7, 26]).

All of which have exceedingly high neutral hydrogen column densities ($N_{\rm HI} \gtrsim 10^{20}$ cm^{-2}).

Regarding the first class, at present, poor frequency coverage and RFI have restricted searches

for 21 cm absorption to 31 DLAs [28][3], with detections in 16 systems. Unfortunately, most of these are at low redshift, with only three detected at $z \sim 2$, all of which with relatively low quality 21 cm spectra [62, 59, 60]. Furthermore, many of the known DLAs were selected from optical spectra, since these give a broad spectral coverage and hence enable a large redshift range to be searched efficiently. Therefore present DLA samples suffer from dust bias, making these poor candidates in which to search for molecules[4]. The high sensitivity and broad spectral coverage of the SKA will enable surveys to be carried out entirely in the radio regime, avoiding all previous dust extinction bias problems (see Kanekar & Briggs, this volume). This will be of particular interest at $z_{\rm abs} \lesssim 1.8$, redshifts where the Lyman-α line cannot be observed by ground-based telescopes[5]: The cold phase of H I is also expected to be more prevalent at lower redshift due to increased star formation, resulting in higher metallicities and thus a larger number of radiation pathways for the gas to cool [28].

Many of the latter two classes are often[6] found toward what are generally referred to as "red quasars". In these, the reddening of the quasar light is believed to be due to the presence of dust along the line of sight to the quasar (e.g. [53]). These are therefore more likely to have high molecular abundances (e.g. [56]) but, due to the dust obscuration, are very difficult objects in which to obtain high resolution optical spectra: Examples of these are the 4 known molecular absorbers (§2.3) of which PKS 1413+135 & B3 1504+377 are associated with the host and B0218+357 & PKS 1830–210 are gravitational lenses: All have background AGNs with colours of $V-K > 5$, while typical bright quasars (including those with intervening DLAs) have far bluer colours, $V - K < 3.4$. In using red quasars, we should bear in mind, however, that:

- Host absorption systems sometimes have strong velocity fields, due to their proximity to the AGN, which may result in various lines arising in regions of differing velocities. It is thus important to obtain multiple estimates in individual sources.

- The structure of the background emitting region can be different between centimetre and millimetre wavelengths; this can be important for gravitational lenses since the light paths of the lines might be quite different. It is thus more prudent to compare lines arising at similar frequencies, such as the 18 cm OH ground state lines.

3.3. Atomic lines

Although millimetre lines are absent in DLAs (see §3.4), and the relative incidence of 21 cm absorption is considerably lower than in red quasars ($\approx 10\%$, cf. $\approx 80\%$ [2]), DLAs and sub-DLAs constitute a large (> 300) sample[7] of high column density ($N_{\rm HI} \gtrsim 10^{20}$ cm^{-2}) absorbers at known redshifts. Of these, although only 31 have been thoroughly searched (§3.2), there are 58 known DLAs and a further 29 sub-DLAs which occult radio-loud quasars, where we define this as ≥ 0.5 Jy, the minimum flux density illuminating a DLA currently detected in 21 cm absorption (see [11]).

For an optically thin, homogeneous cloud, the column density (cm^{-2}) of the absorbing gas is given by

$$N_{\rm HI} = 1.823 \times 10^{18} . \frac{T_{\rm spin}}{f} \int \tau dv \qquad (11)$$

where $T_{\rm spin}$ is the spin temperature of the gas (K), f is the covering factor of the continuum flux and $\int \tau dv$ is the integrated optical depth of the line (km s^{-1}). Applying the 3σ opacities of $\tau \approx 1 - 20 \times 10^{-4}$ obtained after one hour of integration (§3.1) with the SKA, gives $N_{\rm HI} \approx 2 - 20 \times 10^{14} . \frac{T_{\rm spin}}{f}$ cm^{-2} per unit km s^{-1} line-

[3] See [11] for further details.

[4] Also potentially affecting both chemical evolution and number density evolution studies, although radio selected quasars and follow-up optical spectroscopy have been used to partly overcome this problem [18].

[5] Note that current DLA samples contain hardly any systems in the redshift range $0.7 < z_{\rm abs} < 1.8$ [46].

[6] Although not always. For example, [51] find 21 cm absorption in the hosts of 19 compact radio sources at $z \leq 0.85$, where the covering factor (Equation 11) is high.

[7] Comprising of 150 confirmed DLAs (e.g. [46]) and > 150 sub-DLAs/candidate systems.

width[8, 9] over $z_{\rm abs} = 0 - 6$. For $T_{\rm spin} \approx 100$ K, a ~ 10 km s^{-1} wide[10] 21 cm absorption line, at 1 km s^{-1} resolution, would be detectable to $N_{\rm HI} \gtrsim 10^{17}$ cm^{-2} after one hour. That is, for the first time in Lyman-limit systems, thus increasing the number of potential 21 cm absorbers for which the redshifts are currently available by 3 orders of magnitude. For DLAs (where $N_{\rm HI} \geq 2 \times 10^{20}$ cm^{-2}) we obtain the limit $\frac{T_{\rm spin}}{f} \gtrsim 10^4$ K (~ 10 km s^{-1} line-width), thus covering a large range of spin temperatures and covering factors in the known systems which occult radio-loud quasars[11]. Immediately, this increases the number of possible 21 cm absorbing DLAs and sub-DLAs by a factor of 5 in the systems currently known. Furthermore, these limits significantly improve the potential of finding absorption in those DLAs much more weakly illuminated at radio frequencies.

With the high quality spectra obtained from the high column density absorbers, Voigt profile fitting to the line shape can then be used to measure the line strength to a fraction of the channel width, suggesting that even such "detection" experiments could obtain a redshift precision of $\Delta z \approx 3 \times 10^{-6}$. Clearly, in reasonable integration times, the SKA should be able to measure the 21 cm line redshift to a precision of better than $\sim 10^{-6}$ for all ≈ 50 DLAs of the current $z \gtrsim 2$ sample.

Similar accuracies of 10^{-6} are also possible from measurements of the redshifts of optical resonance lines in these DLAs. However, systematic offsets between the velocities of the optical and 21 cm lines are likely to dominate the error estimates on individual systems, which could be of order 5 – 10 km s^{-1}, due to small scale motions in the ISM. Assuming a dispersion of $\approx$ 3 km s^{-1} between the optical and 21 cm redshifts, implies an additional redshift error of $\sim 10^{-5}$, far larger than the measurement error. However, even with only 21 cm detections in the 50 DLAs of the current $z \gtrsim 2$ sample, a large increase in precision is obtained: For an assumed median redshift of 2.5, the 1σ sensitivity to changes in $\Delta x/x = 4 \times 10^{-7}$. Note that the quadratic dependence of x on α implies that the sensitivity to a variation in α is already comparable to the sensitivity of the Oklo measurement (§1).

3.4. Molecular lines

As mentioned previously (§3.2), by using optically selected objects, such as DLAs, we are selecting against dusty (i.e. visually obscured) objects which are more likely to harbour molecules in abundance (e.g. [19, 33]). In fact, the DLAs in which H_2 has been detected ($\approx 10\%$ of the sample), have molecular hydrogen fractions, $\mathcal{F} \equiv 2N(H_2)/[2N(H_2) + N(\mathrm{H\,I})]$, in the range $-6 < \log_{10}\mathcal{F} < -2$ [33]. These optical searches are generally limited to above the atmospheric cut-off of the Lyman and Werner H_2-bands in the UV ($z_{\rm abs} \gtrsim 1.8$). However, although not as sensitive as in the optical domain, searches for absorption in the rotational transitions of CO and HCO^+ show that molecular fractions of $\log_{10}\mathcal{F} \lesssim -1$ are expected at low redshift (see [12] and references therein). These low molecular fractions are not surprising given that these samples are drawn from flux-limited optical surveys. Surveys for 21 cm absorption with the SKA will, however, give rise to samples of "DLAs" unbiased by dust extinction; some of these are likely to have reasonable molecular fractions, yielding many systems with detections of both H I and molecular lines.

3.4.1. Millimetre transitions

With its frequency cut-off of 25 GHz, the SKA will be able to observe the strongest absorbing molecules detected in the 4 known systems, HCN, HCO^+ and CO, at $z_{\rm abs} \gtrsim 2.6$. At the low end of this range, a one hour integration

[8] Note that for a single cloud in thermodynamic equilibrium, the spin temperature is approximately equal to the kinetic temperature of the gas, giving $T_{\rm s} \approx 22 \times \mathrm{FWHM}^2$. That is, for $T_{\rm spin} \geq 100$ K the line-width (FWHM) is expected to be ≥ 2 km s^{-1}.

[9] Since for continuum fluxes of $S > 0.05$ Jy, the antenna temperature exceeds the receiver temperature of the SKA, this estimate will hold for all values significantly greater than this as $T_{\rm sys} = T_{\rm ant} + T_{\rm rec} \propto S$ and $\tau \approx \frac{\sigma}{S}$ ($\tau << 1$).

[10] In the case of H I these can be $\approx 4 - 50$ km s^{-1} in DLAs ([61, 32]) and $\approx 15 - 100$ km s^{-1} in red quasars (e.g. [2]).

[11] The redshifted frequencies of many of these make them inaccessible to current telescopes.

at 1 km s^{-1} resolution gives a 3σ opacity of $\tau \approx 3 \times 10^{-4}$ (§3.1) for background continuum flux of 0.1 Jy. For rotational lines the total column density of each molecule is given by

$$N_{\rm mol} = \frac{8\pi}{c^3} \frac{\nu^3}{g_{J+1} A_{J+1\rightarrow J}} \frac{Q e^{E_J/kT_{\rm x}}}{1 - e^{-h\nu/kT_{\rm x}}} \int \tau dv \quad (12)$$

where ν is the rest frequency of the $J \rightarrow J+1$ transition, g_{J+1} and $A_{J+1\rightarrow J}$ are the statistical weight and the Einstein A-coefficient of the transition, respectively, $Q = \sum_{J=0}^{\infty} g_J \ e^{-E_J/kT_{\rm x}}$ is the partition function, for the excitation temperature, $T_{\rm x}$, and $\int \tau dv$ is the upper limit of the velocity integrated optical depth of the line. Assuming a typical "dark cloud" excitation temperature of $T_{\rm x} \gtrsim 20$ K (i.e. 10 K at $z = 0$), the SKA will give column density sensitivities of $N_{\rm CO} \approx 6 \times 10^{12}$ cm^{-2}, $N_{\rm HCO+} \approx 5 \times 10^9$ cm^{-2} and $N_{\rm HCN} \approx 10^{10}$ cm^{-2} per unit line-width[12] after one hour of integration.

In terms of sensitivity, these limits are comparable to the current optical (CO electronic) searches in DLAs (see [12])[13], and due to the steep molecular fraction evolution in these objects [13], the detection of millimetre transitions is expected to remain beyond our grasp. However, for $N_{\rm HI} \gtrsim 10^{20}$ cm^{-2} and $N_{\rm H_2} \sim 10^4 N_{\rm CO}$ (again for dark clouds, e.g. [54]), we obtain sensitivities to molecular fractions of $\mathcal{F} \gtrsim 10^{-4}$ (or $\mathcal{F} \gtrsim 10^{-2}$ using the, perhaps more reliable [36], conversion of $N_{\rm HCO^+} = 2 - 3 \times 10^{-9} N_{\rm H_2}$), cf. $\mathcal{F} = 0.3 - 1.0$ for the 4 known millimetre systems (e.g. [9]). Note that since these estimates are per unit line-width the sensitivities will decrease directly as the FWHM of the line[14].

One foreseeable problem is the possibility of any cosmological evolution in the molecular hydrogen fraction: According to [13], H_2-bearing DLAs exhibit a steep decrease in relative molecular hydrogen abundance with redshift. If such a trend generally exists, due to the restriction of searching for $z_{\rm abs} \gtrsim 2.6$ millimetre absorption, the full sensitivity of $\mathcal{F} \lesssim 10^{-4}$ may be required[15]. This problem may be circumnavigated by searching for centimetre lines at $z_{\rm abs} \lesssim 2.6$, which we discuss next.

3.4.2. OH lines

Although restrictive in its redshift coverage of millimetre lines, at centimetre wavelengths many times as many sources at a given flux density are expected than at higher frequencies. Additionally, since the instantaneous bandwidth is a quarter of the band centre frequency, complete searches for 18 cm OH to $z \lesssim 16$ can be performed in relatively few scans. This combined with the large field of view at low frequencies, makes the SKA the ideal instrument with which to perform blind searches for OH absorption.

For an optically thin cloud in thermal equilibrium, the OH column density is related to the excitation temperature and 1667 MHz optical depth by (e.g. [45])

$$N_{\rm OH} \approx 2.38 \times 10^{14} . \frac{T_{\rm x}}{f} \int \tau dv \quad (13)$$

which, again for a flux density of 0.5 Jy, gives a 3σ sensitivity of $N_{\rm OH} \approx 3 - 30 \times 10^{10} \frac{T_{\rm x}}{f}$ cm^{-2} over $z_{\rm abs} = 0 - 7$, per km s^{-1} line-width. Since the line-widths can range anywhere from $\approx 10 - 200$ km s^{-1} in the 4 known systems (§2.3), pessimistically *very high resolution* spectra of very wide lines will be detected by the SKA to $N_{\rm OH} \sim 10^{13} \frac{T_{\rm x}}{f}$ cm^{-2}, cf. $N_{\rm OH} \sim 1 - 12 \times 10^{14} \frac{T_{\rm x}}{f}$, currently detected at *low resolution* in the known systems ($z_{\rm abs} \leq 0.9$).

For $N_{\rm OH} \approx 30 N_{\rm HCO^+}$ (§2.2.2) and using the $N_{\rm HCO^+}$–$N_{\rm H_2}$ conversion ratio quoted above, gives a sensitivity to $\mathcal{F} \gtrsim 10^{-2}$ after one hour, in the low redshift regime. Since redshifts of $z_{\rm abs} \lesssim 2.6$ can be observed in OH 18 cm, any molecular fraction evolution is of considerably less consequence than in the millimetre case.

[12] The 4 known redshifted millimetre absorbers (§2.3) have line-widths $\lesssim 20$ km s^{-1}.

[13] Note that, using the UV Werner band, optical CO searches are restricted to $z_{\rm abs} \gtrsim 1.6$, cf. $z_{\rm abs} \gtrsim 3.6$ with the SKA.

[14] For example, in a detection experiment, where a resolution (and FWHM) of 10 km s^{-1} may be used, these sensitivities would decrease by a factor of $\leq \sqrt{10}$.

[15] Also, for a given velocity resolution the sensitivity decreases as the square root of the observed frequencies (§3.1) further compounding the difficulty of detecting molecules at high redshift.

Table 1
Summary of the various combinations of fundamental constants which can be constrained from various spectral lines, where g_p is the proton g-factor, $\alpha \equiv e^2/\hbar c$ is the fine structure constant and $\mu \equiv m_e/m_p$ the ratio of electron/proton masses.

Transition	"Anchor"	Constrained quantity
H I 21cm	Metal-ion (optical)	$g_p\mu\alpha^2$
	HCO^+	$g_p\alpha^2$
	OH 18cm ($\nu_{1665}+\nu_{1667}$)	$g_p[\alpha^2/\mu]^{1.57}$
OH 18cm ($\nu_{1665}+\nu_{1667}$)	HCO^+	$\mu^{1.57}\alpha^{-1.14}$
	OH 18cm ($\nu_{1665}-\nu_{1667}$)	$g_p[\alpha^2/\mu]^{0.13}$
	OH 18cm ($\nu_{1720}-\nu_{1612}$)	$g_p[\alpha^2/\mu]^{1.85}$
	OH 6cm	$[\alpha^2/\mu]^{-2.06}$

4. SUMMARY

To summarise, with its high sensitivity, wide field of view and broad frequency coverage (unaffected by RFI), the SKA will revolutionize radio studies of the cosmological evolution of various fundamental constants (see Table 1). The SKA will be unparalleled in detecting these lines in:

- Optically selected QSO absorbers: Being of low dust content these sources are best targeted for 21 cm absorption. In this transition, the SKA truly excels and we expect detections in systems with column densities as low as $N_{\rm HI} \sim 10^{17}$ cm^{-2} (i.e. Lyman limit systems) or in DLAs with spin temperature/covering factor ratios as high as $\frac{T_{\rm spin}}{f} \sim 10^4$. Even with the currently known redshifted optical absorption systems, this will increase the number of known 21 cm absorbers many-fold.

- Red quasars: Being visually obscured these objects provide the best targets for molecular absorption searches, but are, by definition, currently much rarer in current searches than optical absorbers. However, with its extremely wide band-width and field of view, the SKA has the potential to discover many more systems invisible to optical surveys, via the H I 21 cm and OH 18 cm lines.

Currently there are only 4 redshifted radio molecular absorbers known. The discovery of more of these systems will prove invaluable in studying the physics and chemistry of the early Universe. Furthermore, molecular absorption lines are extremely important in constraining fundamental constants since:

  - The spectral resolution available in radio spectroscopy is generally much better than the optical, thus giving a measurement better matched for comparison with the H I line. This will allow estimates of $\Delta x/x \sim few \times 10^{-7}$ ($x \equiv g_p\mu\alpha^2$).
  - These transitions allow the contribution of the proton g-factor to be separated out and give more combinations with which to determine the relative contribution of each constant to any measured change (Table 1). Although the frequency coverage will exclude the detection of millimetre absorption below redshifts of $z_{\rm abs} \approx 2.6$, it will excel in finding OH which will provide a diagnostic with which to find HCO^+ with higher frequency telescopes such as ALMA.

It is therefore seen that these much improved statistics applied to the various combinations of

fundamental constants available will permit measurements of the cosmological evolution of each the fine structure constant, the ratio of electron–proton mass and the proton g-factor. Through measurements of these combinations of constants in the early Universe, the SKA could provide the means of experimentally testing current Grand Unified Theories.

References

[1] Carilli, C. L., Menten, K. M., Reid, M. J., & Rupen, M. P. 1997, Astrophys. J., 474, L89

[2] Carilli, C. L., Menten, K. M., Reid, M. J., Rupen, M. P., & Yun, M. S. 1998, Astrophys. J., 494, 175

[3] Carilli, C. L., Menten, K. M., Stocke, J. T., Perlman, E., Vermeulen, R., Briggs, F., de Bruyn, A. G., Conway, J., & Moore, C. P. 2000, Phys. Rev. Lett., 85, 5511

[4] Carilli, C. L., Perlman, E. S., & Stocke, J. T. 1992, Astrophys. J., 400, L13

[5] Carilli, C. L., Rupen, M. P., & Yanny, B. 1993, Astrophys. J., 412, L59

[6] Chand, H., Srianand, R., Petitjean, P., & Aracil, B. 2004, Astr. Astrophys., 417, 853

[7] Chengalur, J. N., de Bruyn, A. G., & Narasimha, D. 1999, Astr. Astrophys., 343, L79

[8] Chengalur, J. N. & Kanekar, N. 2003, Phys. Rev. Lett., 91, 241302

[9] Combes, F. & Wiklind, T. 1998, ESO Messenger, 91, 29

[10] Cowie, L. L. & Songaila, A. 1995, Astrophys. J., 453, 596

[11] Curran, S. J., Murphy, M. . T., Pihlström, Y. M., Webb, J. K., & Purcell, C. R. 2004, Mon. Not. R. astr. Soc., in press (astro-ph/0410647)

[12] Curran, S. J., Murphy, M. T., Pihlström, Y. M., Webb, J. K., Bolatto, A. D., & Bower, G. C. 2004, Mon. Not. R. astr. Soc., 352, 563

[13] Curran, S. J., Webb, J. K., Murphy, M. T., & Carswell, R. F. 2004, Mon. Not. R. astr. Soc., 351, L24

[14] Damour, T. & Polyakov, A. M. 1994, Nucl. Phys. B, 423, 596

[15] Darling, J. 2003, Phys. Rev. Lett., 91, 011301

[16] Drinkwater, M. J., Webb, J. K., Barrow, J. D., & Flambaum, V. V. 1998, Mon. Not. R. astr. Soc., 295, 457

[17] Dzuba, V. A., Flambaum, V. V., & Webb, J. K. 1999, Phys. Rev. A, 59, 230

[18] Ellison, S. L., Yan, L., Hook, I. M., Pettini, M., Wall, J. V., & Shaver, P. 2001, Astr. Astrophys., 379, 393

[19] Fall, S. M. & Pei, Y. C. 1993, Astrophys. J., 402, 479

[20] Fujii, Y., Iwamoto, A., Fukahori, T., Ohnuki, T., Nakagawa, M., Hidaka, H., Oura, Y., & Möller, P. 2000, Nucl. Phys. B, 573, 377

[21] Hill, C. T. & Ross, G. C. 1988, Nucl. Phys. B, 311, 253

[22] Ishwara-Chandra, C. H., Dwarakanath, K. S., & Anantharamaiah, K. R. 2003, J. Astrophys. Astr., 24, 37

[23] Ivanchik, A., Petitjean, P., Rodriguez, E., & Varshalovich, D. 2003, Astrophys. Space Sci., 283, 583

[24] Jones, D. L. 2004, SKA Memo 45

[25] Kanekar, N., Athreya, R. M., & Chengalur, J. N. 2002, Astr. Astrophys., 382, 838

[26] Kanekar, N. & Briggs, F. H. 2003, Astr. Astrophys., 412, L29

[27] Kanekar, N. & Chengalur, J. N. 2002, Astr. Astrophys., 381, L73

[28] Kanekar, N. & Chengalur, J. N. 2003, Astr. Astrophys., 399, 857

[29] Kanekar, N. & Chengalur, J. N. 2004, Mon. Not. R. astr. Soc., 350, L17

[30] Kanekar, N., Chengalur, J. N., & Ghosh, T. 2004, Phys. Rev. Lett., 93, 051302

[31] Lamoreaux, S. 2003, nucl-th/0309048

[32] Lane, W. M. & Briggs, F. H. 2001, Astrophys. J., 561, L27

[33] Ledoux, C., Petitjean, P., & Srianand, R. 2003, Mon. Not. R. astr. Soc., 346, 209

[34] Li, L.-X. & Gott, J. R. 1998, Phys. Rev. D, 58, 103513

[35] Liszt, H. & Lucas, R. 1996, Astr. Astrophys., 314, 917

[36] Liszt, H. S. & Lucas, R. 2000, Astr. Astrophys., 355, 333

[37] Marciano, W. 1984, Phys. Rev. Lett., 52, 489

[38] Marion, H., Santos, F. P. D., Abgrall, M., Zhang, S., Sortais, Y., Bize, S., Maksimovic, I., Calonico, D., Gruenert, J., Mandache, C., Lemonde, P., Santarelli, G., Laurent, P., Clairon, A., & Salomon, C. 2003, Phys. Rev. Lett., 90, 150801

[39] Moore, C. B., Carilli, C. L., & Menten, K. M. 1998, Astrophys. J., 510, L87

[40] Murphy, M. T., Webb, J. K., & Flambaum, V. V. 2003, Mon. Not. R. astr. Soc., 345, 609

[41] Murphy, M. T., Webb, J. K., Flambaum, V. V., Churchill, C. W., & Prochaska, J. X. 2001, Mon. Not. R. astr. Soc., 327, 1223

[42] Murphy, M. T., Webb, J. K., Flambaum, V. V., Drinkwater, M. J., Combes, F., & Wiklind, T. 2001, Mon. Not. R. astr. Soc., 327, 1244

[43] Murphy, M. T., Webb, J. K., Flambaum, V. V., Prochaska, J. X., & Wolfe, A. M. 2001, Mon. Not. R. astr. Soc., 327, 1237

[44] Olive, K. A., Pospelov, M., Qian, Y.-Z., Manhès, Vangioni-Flam, E., Coc, A., & Cassé, M. 2004, Phys. Rev. D, 69, 027701

[45] Plume, R., Kaufman, M. J., Neufeld, D. A., Snell, R. L., Hollenbach, D. J., Goldsmith, P. F., Howe, J., Bergin, E. A., Melnick, G. J., & Bensch, F. 2004, Astrophys. J., 605, 247

[46] Prochaska, J. X., Gawiser, E., Wolfe, A. M., Cooke, J., & Gelino, D. 2003, Astrophys. J. Suppl. Series, 147, 227

[47] Sandvik, H. B., Barrow, J. D., & Magueijo, J. 2002, Phys. Rev. Lett., 88, 031302

[48] Srianand, R., Chand, H., Petitjean, P., & Aracil, B. 2004, Phys. Rev. Lett.

[49] Townes, C. & Schawlow, A. 1955, Microwave Spectroscopy (U.S.A.: McGraw-Hill)

[50] Uson, J. M., Bagri, D. S., & Cornwell, T. J. 1991, Phys. Rev. Lett., 67, 3328

[51] Vermeulen, R. C., Pihlström, Y. M., Tschager, W., de Vries, W. H., Conway, J. E., Barthel, P. D., Baum, S. A., Braun, R., Bremer, M. N., Miley, G. K., O'Dea, C. P., Roettgering, H. J. A., Schilizzi, R. T., Snellen, I. A. G., & Taylor, G. B. 2003, Astr. Astrophys., 404, 861

[52] Webb, J. K., Flambaum, V. V., Churchill, C. W., Drinkwater, M. J., & Barrow, J. D. 1999, Phys. Rev. Lett., 82, 884

[53] Webster, R. L., Francis, P. J., Peterson, B. A., Drinkwater, M. J., & Masci, F. J. 1995, Nature, 375, 469

[54] Wiklind, T. & Combes, F. 1995, Astr. Astrophys., 299, 382

[55] —. 1996, Astr. Astrophys., 315, 86

[56] Wiklind, T. & Combes, F. 1996, in Science with Large Millimetre Arrays, Proceedings of the ESO-IRAM-NFRA-Onsala Workshop, ed. P. Shaver (Berlin: Springer-Verlag), 86

[57] —. 1997, Astr. Astrophys., 328, 48

[58] —. 1998, Astrophys. J., 500, 129

[59] Wolfe, A. M., Briggs, F. H., & Jauncey, D. L. 1981, Astrophys. J., 248, 460

[60] Wolfe, A. M., Briggs, F. H., Turnshek, D. A., Davis, M. M., Smith, H. E., & Cohen, R. D. 1985, Astrophys. J., 294, L67

[61] Wolfe, A. M., Broderick, J. J., Condon, J. J., & Johnston, K. J. 1978, Astrophys. J., 222, 752

[62] Wolfe, A. M. & Davis, M. M. 1979, Astron. J., 84, 699

[63] Wu, Y. & Wang, Z. 1986, Phys. Rev. Lett., 57, 1978